heritage

MDPI

Article

Preserving Intangible Heritage through Tangible Finds: The "Skull with Ears"—St. Luciella ai Librai's Church (Naples, Italy)

Andrea Macchia [1,*], Stefania Montorsi [1], Giorgia Salatino [1], Romana Albini [1], Eugenio Cerilli [1], Chiara Biribicchi [1], Massimo Faella [2], Angela Rogliani [2], Tilde de Caro [3], Carmine Lubritto [4], Carmela Vetromile [4], Maria Rosa Di Cicco [4], Andrea Ambrosini [1] and Alessandra Sperduti [5]

1 YOCOCU, Youth in Conservation of Cultural Heritage, Via T. Tasso 108, 00185 Rome, Italy; chiara.biribicchi@uniroma1.it (C.B.)
2 Respiriamo Arte, Vico Santa Luciella ai Librai 5, 80138 Naples, Italy
3 CNR-ISMN, Strada Provinciale 35 d n. 9, 00010 Rome, Italy
4 Department of Environmental, Biological and Pharmaceutical Sciences and Technologies, University of Campania "Luigi Vanvitelli", Via Vivaldi 43, 81100 Caserta, Italy
5 Museo delle Civiltà, P.zza Guglielmo Marconi 14, 00144 Rome, Italy
* Correspondence: andrea.macchia@uniroma1.it

Abstract: The present study reports the conservative first aid concerning the human cranium known as the "Skull with Ears", which is conserved in the crypt of Santa Luciella ai Librai's church in Naples, Italy. These remains have historically been worshipped by devotees within the cult of the "abandoned souls". The skulls were "adopted" by the Neapolitan population and treated with particular care in exchange for divine favors. The critical preservation status of the "Skull with ears" required a multidisciplinary approach aimed at defining the taphonomy and anthropological features of the cranium, while determining the state of its conservation by using a multi-analytical approach. Multispectral imaging, 3D modeling, X-ray imaging, microscopical observations, and microbiological tests enabled the documentation of the cranium while assessing this state of conservation. Electron scanning microscopy (SEM), energy dispersive spectroscopy (EDS), Fourier-transform infrared spectroscopy (FTIR) in the attenuated total reflectance (ATR) mode, and radiocarbon dating allowed for essential data to be obtained on the cranium's history and constituent components. The results that were obtained from both the analysis of the cranium and the environmental monitoring of the crypt showed the advanced degradation of the bones due to a significant bacterial attack, which was facilitated by the inadequate environmental conditions at the site of conservation. The acquired data enabled the definition of the most suitable conservation strategy and the securing of the cranium.

Keywords: skull; conservation; 3D documentation; SEM/EDS; FT-IR ATR; radiocarbon dating; digital microscopy; multispectral imaging; anthropology

Citation: Macchia, A.; Montorsi, S.; Salatino, G.; Albini, R.; Cerilli, E.; Biribicchi, C.; Faella, M.; Rogliani, A.; de Caro, T.; Lubritto, C.; et al. Preserving Intangible Heritage through Tangible Finds: The "Skull with Ears"—St. Luciella ai Librai's Church (Naples, Italy). *Heritage* **2023**, *6*, 3541–3566. https://doi.org/10.3390/heritage6040188

Academic Editors: Arlen F. Chase and Manuela Vagnini

Received: 31 January 2023
Revised: 27 March 2023
Accepted: 3 April 2023
Published: 4 April 2023

1. Introduction

Considering their strong symbolic value, human skulls are at the center of ceremonies, manipulations, representations, and performances among human societies [1]. The rich historical and ethnographic records suggest that the practices and cultural implications that are associated with skull worship can be the most diverse, with changing and fluid meanings even within the same community. They may range between the loss, affirmation, and renegotiation of identities, playing a role in the personal involvement and shared "memory" of communities.

Within cults and rituals, skulls can assume new identities and specific powers of action, both as subjects participating in social life and as mediums between the world of the living and the dead [2]. In this realm, the Neapolitan tradition of the cult of Abandoned Souls ("Anime Pezzentelle") lies. The remains ("capuzzelle", small heads) of nameless people were adopted by the Neapolitans in a reciprocal relationship: the dead functioned

as intermediaries for invocations and requests; in return, the living's prayers soothed the pain of the souls that were relegated to Purgatory and assured a faster transit to Paradise. The cult of Abandoned Souls was developed and practiced in various sites and crypts located in the city of Naples [3], including the Church of Santa Luciella. In 1969, the Roman Catholic Church officially abolished the skull cult, claiming that it incorporated elements of paganism and superstition. Nevertheless, several Neapolitan families still maintain these devotional practices, also involving younger generations [4].

The church of Santa Luciella is a small, ancient building at the end of the little alley "Vico Santa Luciella" (Vicus Cornelianus), connecting San Biagio dei Librai and San Gregorio Armeno. The church was founded in 1327 by Bartolomeo di Capua, a council member for Charles II of Anjou. By the 17th century, the church began to be attended by the Neapolitan stonemasons, who dedicated it to Santa Lucia, the protector of sight. Indeed, these workers frequently risked damaging their eyes, as stone chips could get into the eyes while splintering the stones.

The church was the setting for a particular funerary practice that was prevalent in Naples, but also present in other parts of Italy until the second half of the 19th century [5,6]. Its hypogeum was specifically designed for the ritual of processing the corpses of the confraternity members through an elaborated treatment involving a "double burial". Along its walls, the hypogeum still preserves four *giardinetti* and five niches (*scolatoi*) that hosted these bodies during the whole decomposition process, until they were completely skeletonized. The *giardinetti* were basins filled with soil in which the corpses were superficially buried for the first phase of decomposition; they were then moved to the niches to completely get rid of their soft tissues. The obtained skeletal remains were treated differently, with the postcranial elements being deposited in ossuaries—i.e., pits closed by a grate—whereas the skulls were mostly displayed on the masonry shelves as a symbol of the successful liberation of the soul [5,6]. The acknowledged strong emotional and symbolic charge of this Neapolitan ritual for the deceased evokes Van Gennep's view of the three-stage rites of passage, i.e., separation, transition, and incorporation—the latter when the deceased acquires a new social status [7].

As a result of this practice, the crypt of Santa Luciella's church preserves the remains of around forty skulls, arranged on shelves that have been the object of care and devotion since the 17th century by the ecclesiastic corporation of "Pipernieri". In this cultural setting, the "Skull with Ears" has played a role of considerable importance, since its misaligned and deformed temporal bones—mistaken as mummified ears—led devotees to believe that the skull was able to listen and satisfy their demands more than the other ones. Thus, this object of devotion is directly tied to the Neapolitan intangible heritage, as a manifestation of their collective cultural identity.

In March 2022, YOCOCU APS was entrusted by Respiriamo l'Arte (two private Italian organizations working in the conservation and valorization of cultural heritage) to plan and conduct an interdisciplinary project aimed at defining the conservation state of and a first aid strategy for securing the "Skull with Ears". The aim of the study was twofold: the definition of the taphonomy and anthropological description of its cranium, and the determination of its state of conservation by using a multi-analytical approach and photographic and 3D documentation, both before and after the intervention. The collected data allowed them to address the first restoration aid of the "Skull with Ears", while creating a temporary support to safely exhibit the object in its original collocation.

In addition, the microclimatic conditions of the crypt were monitored from March to September 2022. Indeed, microclimate and multi-parameter monitoring technologies, which have exploded in the last decade, mainly for energy efficiency actions, now find applications in the field of cultural heritage conservation as well [8–10]. In this case study, the information about the environmental conditions of the crypt represents a requirement for defining the most suitable conservation strategy for the skull [11,12].

Ethical Statement

The analysis of and intervention for the "Skull with ears" were explicitly aimed at its preservation, to assure its integrity while maintaining it in the site where it has been stored and displayed for decades. Thus, no ethical issues arose from the research, as it met the demands rather than conflicting with the cultural and religious sensitivities of the devotee community. Indeed, even the Church has shown an increased interest in the scientific analyses of its relics, including the human bodies and skeletons of historical figures [13]. The intervention met the requirements of the Italian Cultural Heritage and Landscape Code (D. Lgs No. 42 of 22 January 2004), which includes human remains—within particular contexts—among the findings that have cultural and identity value. Human remains, thus framed as part of Italy's cultural heritage, are fully protected by law and should be studied and preserved for future generations, like other cultural categories. Indeed, the Code (art. 29) states: "The conservation of Cultural Heritage is ensured through coherent, coordinated, and planned activities of study, prevention, maintenance, and restoration. Prevention means activities suitable for limiting risk situations related to the cultural property in its context. Maintenance means the set of activities and interventions aimed at controlling the condition of the cultural asset and maintaining the integrity, functional efficiency, and identity of the asset and its parts. Restoration means a direct intervention on the property through a complex of operations aimed at the material integrity and recovery of the heritage, protection, and transmission of its cultural values". In addition, the Ministry of Cultural Heritage provides for and supports the cataloging of human remains for cognitive and conservation purposes. The Ministry has also recently published specific guidelines for their proper management—from excavation to museum display—stressing the informative value of such finds, and that all interventions should consider the sensitivity and personal involvement of any possible descendants or related communities [14]. In this regard, it should be underlined that the "Skull with ears" belongs to an anonymous person. Thus, it has no known living descendants.

2. Materials and Methods

2.1. Definition of Conservation State

The cranium's conservation state was investigated through macroscopical and microscopical observations (in visible and ultraviolet light, Dino-Lite AM411-FVW), and multispectral imaging was used to define its extension and type of deposits [15]. The search was carried out with the following spectroscopic techniques [16,17]:

- A Madatec multispectral system consisting of a Samsung NX500 28.2 MP BSI CMOS camera.
- Ultraviolet fluorescence by using Madatec ultraviolet (UV) spotlights (365 nm), a HOYA UV-Infrared (IR) filter cut 52, and a Yellow 495, 52 mm F-PRO MRC 022.
- Infrared reflectography images that were acquired using an 850 nm filter.

The bone tissue fragments recovered near the cranium (spongy and compact tissue fragments from the temporal bones), the incrustations sampled from its surface, and the black deposits from the base of the shelf were sampled and analyzed through electron scanning microscopy (SEM) and energy dispersive spectroscopy (EDS). These SEM-EDS analyses were carried out to observe the morphology of the fragments that were recovered near the cranium, as well as to define the constituent elements of the samples and the possible causes of the deterioration of the cranium. The investigation was carried out on a TESCAN that was equipped with a microprobe X-ray INCA 300 backscattered electron detector (using BSE). The SEM observations were performed in variable pressure mode (VPSEM) on the uncoated samples. The beam accelerating voltage was set between 20 KeV and 30 keV to overcome the critical energy of the electrons to the X-ray emission (a quantitative resolution limit of 0.2% by weight). The carbon percentage was excluded by a semi-quantitative analysis of the EDS spectra that were collected in the environmental conditions.

The FTIR-ATR spectroscopy was carried out both on the salts taken from the cranium and the deposits on the shelf. The IR spectra were collected with the Nicolet Summit FTIR

spectrometer Summit PRO—Thermo Scientific (Waltham, MA, USA) equipped with the Everest ™ Diamond ATR accessory (resolution 8 cm^{-1})—which allows for analyses in the attenuated total reflectance (ATR) mode. In total, thirty-two acquisitions were performed on each sample, and the resulting spectra were then examined using the instrument's library and scientific literature.

The X-ray images were collected using an X-RAY GENERATOR ORANGE 1060 HF to detect the presence of fractured areas that were not visible before the removal of the cranium from the shelf.

Microbiological tests were also conducted to reveal the presence of fungi and/or bacteria. These analyses aimed at assessing the presence of microorganisms that are harmful to humans, since the crypt is often visited by devotees, while evaluating the need for a biocidal treatment during the restoration stage. Plate Count Agar for the total bacterial count and Standard Methods Agar (Plate Count Agar; Tryptone Glucose Yeast Agar) were used to obtain the microbial plate counts from the cranium. Moreover, a cetrimide agar was used to count the *Pseudomonas aeruginosa*, a Gram-negative environmental species. It was selected as a target bacterium because it is the type of *Pseudomonas* that most frequently causes infections in humans [18]. Additionally, it is commonly found in the environment, such as in soil and water [19].

Radiocarbon dating and a stable isotope analysis were performed. The skeletal remains were processed through the isolation of the organic phase of the bone (collagen) by adopting a modified procedure from the Longin method [20]. A sample fragment of about 0.5–1 g was selected, and the bone surface was abraded to remove any contaminants. The remains were then placed in demineralized polypropylene test tubes to carry out a sequence of acid attacks with hydrochloride acid (HCl). For this purpose, the tubes were stored in a cooler at 4 °C for several days. Following each step, deionized water was used for rinsing before the samples were dried. Lastly, the gelatinization protocol was applied [9,10]. For the collagen quality tests, the C and N fractions of the collagen dry mass (C% and N%) were measured via an elemental analyzer (CN Flash EA1112, Thermo Scientific). The samples were retained for isotope analyses. The extracted collagen achieved a yield higher than 1% and an atomic C:N ratio between 2.9 and 3.6 [21–23].

The treated samples underwent graphitization for the accelerator mass spectrometry (AMS) radiocarbon dating, which was performed at the CIRCE Laboratory (Caserta, Italy). The radiocarbon conventional dates were calibrated by using OxCal 4.4 [24] and the recommended calibration curve IntCal20 [25].

Moreover, the stable isotope analyses were realized at the iCONa lab of the University of Campania, using a Delta V Advantage Isotope Ratio Mass Spectrometer coupled with a Flash EA 1112 Elemental Analyser via a ConFlo III interface (Thermo Fisher Scientific). The results were reported in delta notation and calibrated to the international standards VPDB for $\delta^{13}C$ and AIR for $\delta^{15}N$.

The cranium was also analyzed to determine the taphonomy changes and inventory the bones and teeth. The sex, age at death, and health status were defined [26].

Eventually, the microclimate monitoring of the crypt was carried out between March and September 2022, namely from the month before YOCOCU's intervention for the cranium and the month after it. A total of two Hobo U12-012s by Onset USA were used for the measurements of the humidity (RH%), temperature (°C), and luminance (Lux) at the entrance of the crypt and near the site of the collocation of the cranium.

2.2. Documentation and 3D Reconstruction

Detailed and general photographic documentation was acquired using a Nikon D7500 camera and diffuse lighting before the intervention and during the whole process.

3D models of the cranium were created using digital photogrammetry (Metashape 1.7.0, Agisoft—St. Petersburg, Russia), an indirect survey technique which processed the images of the object that were taken from progressive angles, on both the RGB and multispectral

cameras, into high-value spatial information in the form of dense point clouds, textured polygonal models, georeferenced true orthomosaics, and DSMs/DTMs.

These photographic acquisitions were carried out at three different times during the interventions, obtaining the following three-dimensional models:

- Relief 1: a 3D model that was acquired before the safety operation, with the skull in its original position (Figure 1).
- Relief 2: a 3D model that was acquired during the consolidation procedure, after the skull had been overturned and handed.
- Relief 3: a 3D model that was acquired after the consolidation intervention and placement of the skull in the box.

Figure 1. Relief 1, 3D model of the cranium before first aid intervention.

The graphic documentation regarding the conservation status and conservative operations was realized on the acquired 3D models with Procreate®, an App for digital 2D and 3D illustrations that is available for Apple iPad, on an iPad Air 2020.

2.3. First Aid Intervention

The concept of "minimum intervention" guided all the operations on the cranium. Several materials were previously tested in the laboratory to find the best ones that fit the peculiar micro-climatic features of the crypt. The intervention aimed at restoring the material's cohesive properties, in particular around the "ears" area, and designing the temporary support for avoiding direct contact between the cranium and the shelf. The final intent was to redistribute the weight onto the rigid part of the cranium, instead of the weaker structures (such as the fragmented nasal bone).

3. Results

3.1. Crypt Microclimate Monitoring

The crypt housing the skull is single-chambered and connected to the outside by a small window on the street, which was partially closed in April 2022, after the first aid intervention. As a result, its microclimate is humid, with steady R.H. levels corresponding to 99%. Additionally, the temperature ranges from 9 °C to 23 °C. These conditions have severely compromised the preservation of all the crypt's human remains, as well as the "Skull with Ears". Moreover, the walls and the shelves are affected by severe salt crystallizations and the accumulation of dust and deposits of various origins. The data of the two sensors placed in the crypt and near the "Skull with Ears" are reported in Figures 2 and 3.

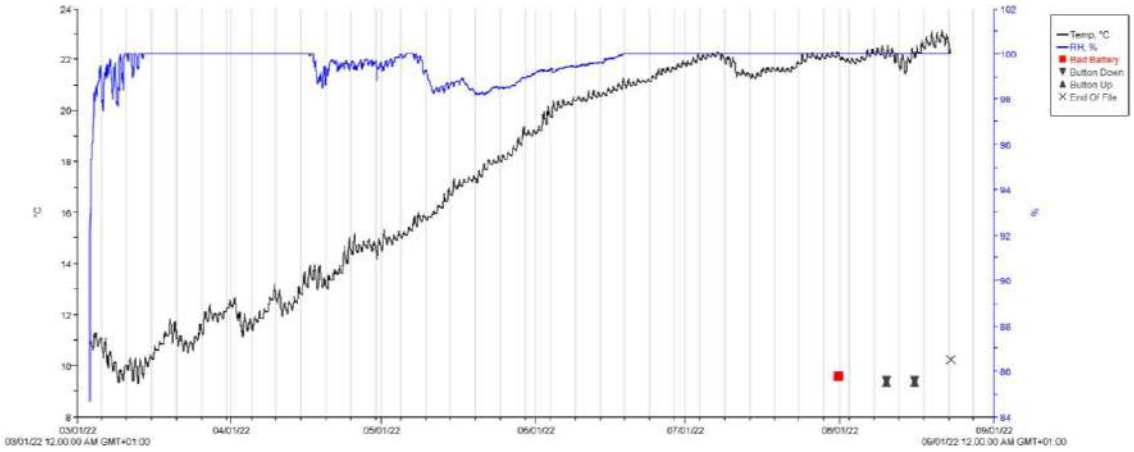

Figure 2. Microclimate monitoring of the crypt. Blue: RH%, and black: temperature (°C).

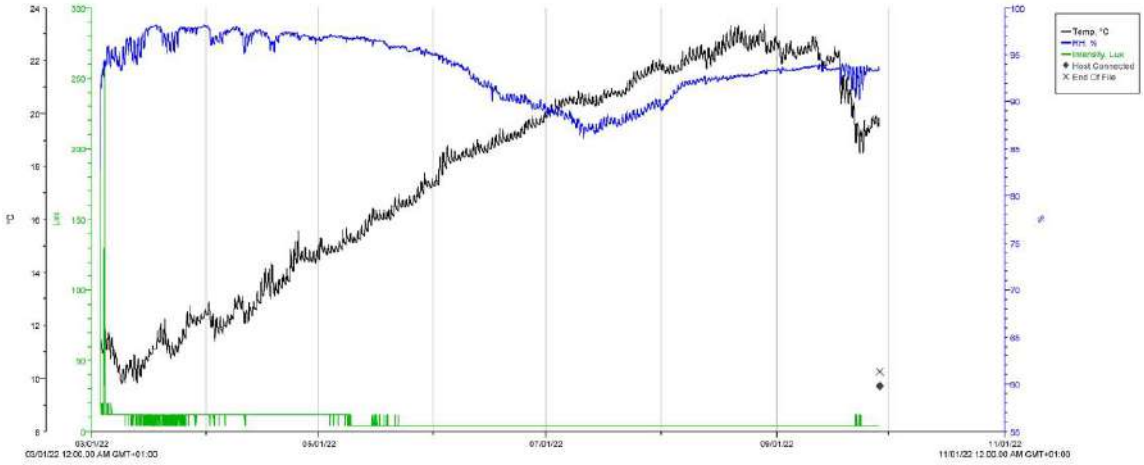

Figure 3. Microclimate monitoring near the site of collocation of the cranium. Blue: RH%, black: temperature (°C), and green: lux.

3.2. Definition of Conservation State

3.2.1. Macroscopic Observations

The conservation state of the "Skull with Ears" before the restoration intervention is shown in Figures 4 and 5. The external surface of the cranium was covered with deposits and grey-blackish encrustations (Figures 6 and 7).

(**a**) (**b**)

Figure 4. The "Skull with Ears" before the study: (**a**) left-side view; and (**b**) top view.

(**a**) (**b**)

Figure 5. The "Skull with Ears" before the study: (**a**) front view; and (**b**) right side.

(**a**) (**b**) (**c**)

Figure 6. Grey crystals on the cranial bones: temporal bone (**a**), top view (**b**), and detail of the surface (**c**).

(**a**) (**b**) (**c**)

Figure 7. Salt crystals on the right temporal bone (**a**,**b**), and right orbit (**c**).

A significant amount of post-mortem deterioration phenomena, such as fractures and flaking, were detected on the bone structure. The cranial vault showed a diffuse and symmetrical porosity, and many areas revealed a "vermicular" alteration, as well as new bone tissue depositions (Figures 8 and 9).

(**a**) (**b**)

Figure 8. State of conservation of the left temporal bone (**a**), and its detail (**b**).

(**a**) (**b**)

Figure 9. State of conservation of the right temporal bone (**a**), and its detail (**b**).

3.2.2. Anthropological Description

The "Skull with Ears" is a partial cranium with complete frontal and parietals, but incomplete occipital and temporal bones. Its splanchnocranium is only represented by nasal bone fragments. Under the neurocranium, small bone fragments and three sparse upper teeth were also recovered: the second and third left molars and the second right molar.

The remains are in poor condition: several areas are covered by coherent and incoherent deposits and grey-blackish encrustations of an allogenic nature; minor and extensive post-mortem fractures and flaking are also visible, especially on the nasal and temporal bones (Figure 10).

(**a**) (**b**)

Figure 10. State of conservation of the nose bones (**a**,**b**).

All the bones appear to be in connection, except for the temporal bones. Over time, these have gradually separated from the parietals at the level of the squamous suture, thus resulting in tilting outwards. The teeth show a flaking of the roots and crowns, with a partial loss of enamel. Some minor concretions are also present.

Based on its morphological features, the cranium belonged to a male individual [26]. The dental wear suggests a mature age at death, approximately between 35 and 50 years [27]. The stages of the sutures obliteration are not fully reliable, as they show a clear discordance. While the sagittal suture appears to be fully fused, the coronal and lambdoid ones are still open. The cranial vault shows a diffuse and symmetrical porosity; many areas reveal "vermicular" alterations, as well as new bone tissue depositions. Given the nonspecific nature of the lesions and the individual's incomplete remains, it is impossible to associate this evidence with a defined pathological condition [28].

3.2.3. Documentation

Tridimensional models have valuable applications in the field of cultural heritage, such as fruition through digital data sharing and reproduction for educational, informative, and conservation purposes.

Some cases have reported the replacement of the original work with a copy, due to either poor conservation or exhibition spaces that were not suitable for proper conservation [29].

Furthermore, this technology is an important aid in the field of conservation and restoration, as a source of documentation and a visual database during the phases of intervention, from the design to the evaluation and from the data analysis to the monitoring.

In the specific case of the "Skull with ears", its state of conservation can be tracked over time by comparing the 3D models that were acquired during the intervention, because it is a complex tridimensional object made of highly degraded organic material. For these reasons, the 3D documentation resulted in being highly appropriate for storing all the data that were collected during the various stages of the study.

2D and 3D tables of graphic documentation on the conservation status and restoration interventions were made. All the post-mortem degradation factors were highlighted directly on the photogrammetric model, which is currently consultable in both static and manipulable formats (Figure 11). This allowed the goal of obtaining high-fidelity graphic documentation without compromising the agility and sustainability, in terms of the consultation and data storage, to be reached.

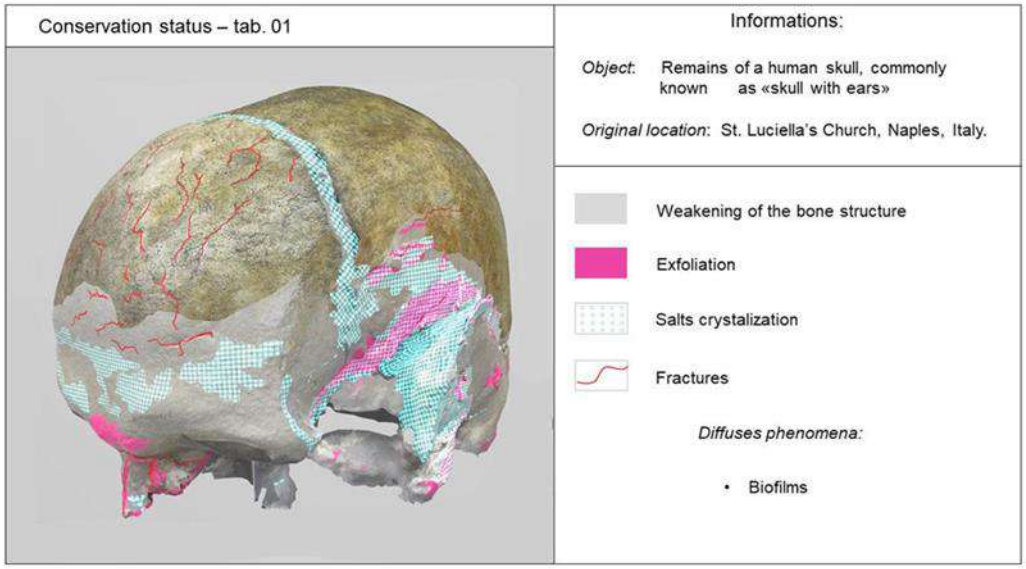

Figure 11. Description of the conservation state of the cranium on its 3D reconstruction.

3.2.4. Analytical Investigations

Multispectral Imaging

The images acquired in the UV fluorescence show patches of yellow fluorescence in the bone tissue, as well as in the areas with no fluorescence, due to superficial deposition (Figure 12). This yellowish fluorescence is related to the organic proteinaceous fractions of the bone, such as amino acids, tyrosine, and tryptophan. Even though it is denatured, the collagen shows a typical fluorescence, the intensity of which decreases as a function of time [15]. No additional information was obtained through IR reflectography.

Digital Microscopy

The surface is characterized by stratified encrustations due to the degradation of the bone tissue and its interaction with environmental dust. The optical microscopical images highlight the presence of white/grey inorganic aggregates on the surface (Figures 13 and 14) and transparent and colorless salts with no UV fluorescence emission (Figures 15 and 16). Besides the diagenetic changes, pathological features can be documented on the skull, such as porotic hyperostosis, which is an overgrowth of the spongy marrow space of the skull (Figure 17), and healing lesions and porosities in the orbital roof (cribra orbitalia) (Figure 18). Eventually, normal physiological features can be detected, such as the attachment of the temporal muscle (Figure 19) and the ectocranial tract of the lambdoid suture (Figure 20).

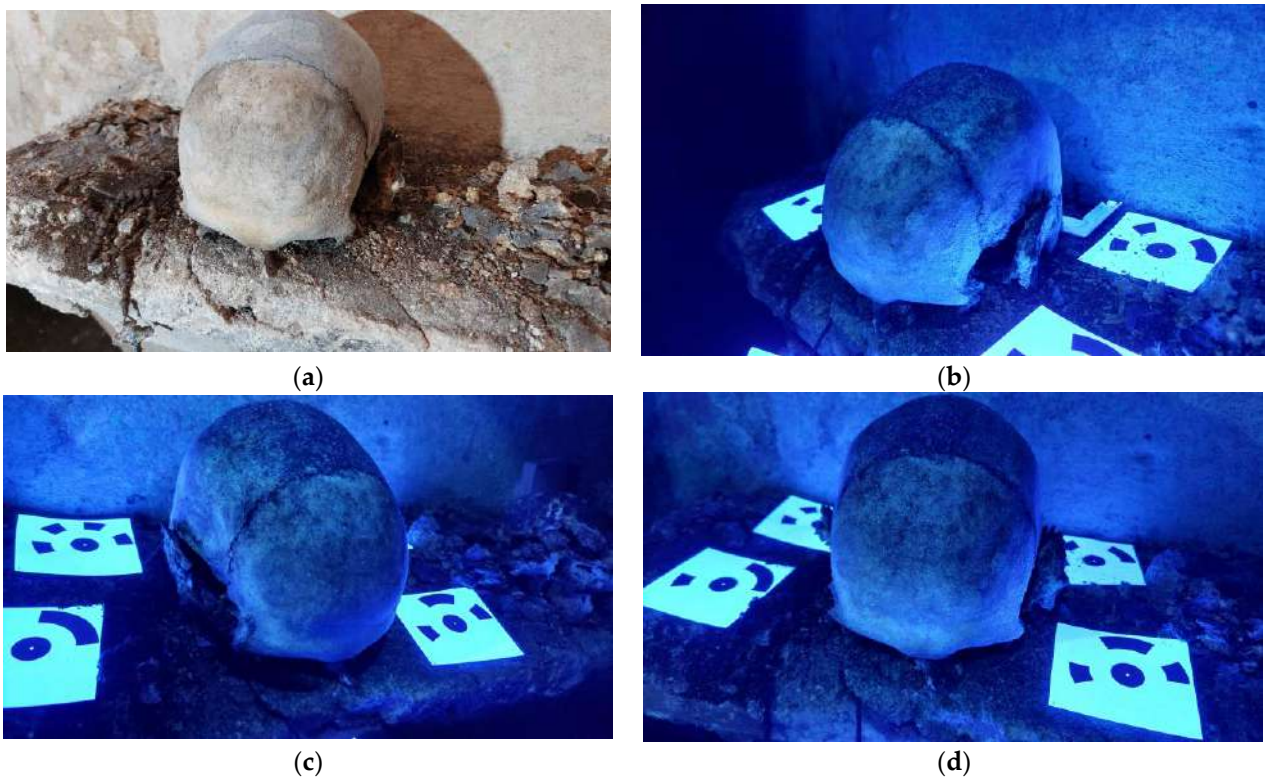

(**a**) (**b**)

(**c**) (**d**)

Figure 12. Images of the "Skull with Ears" in UV fluorescence (**a**–**d**).

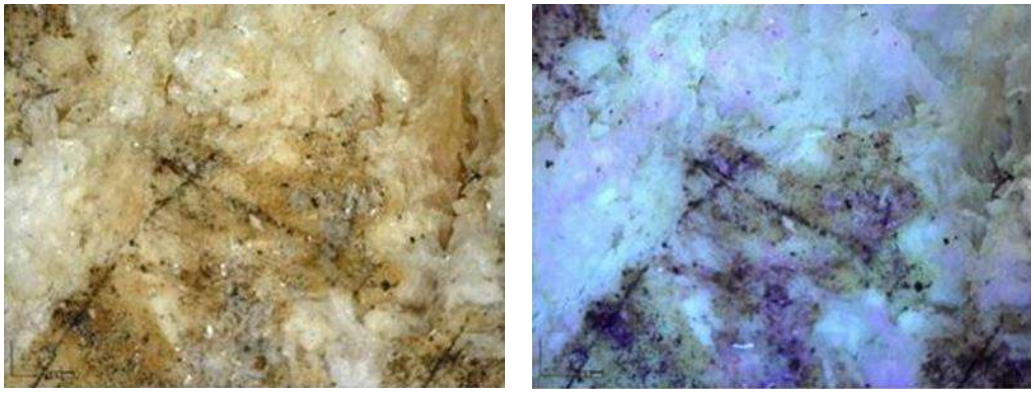

(**a**) (**b**)

Figure 13. Dino-Lite acquisition of the transparent salts present on the cranium surface (220×): (**a**) images in visible light; and (**b**) UV fluorescence micrographs.

Electron Scanning Microscopy (SEM) and Energy Dispersive Spectroscopy (EDS)

The following samples were analyzed through electron scanning microscopy (SEM) and energy dispersive spectroscopy (EDS): (a) the spongy and (b) compact tissue fragments from the temporal bones; (c) the salts from the cranium surface; and (d) the black deposits from the base of the shelf.

(**a**) (**b**)

Figure 14. Dino-Lite acquisition of the white salts present near the right temporal bone (220×): (**a**) images in visible light; and (**b**) UV fluorescence micrographs.

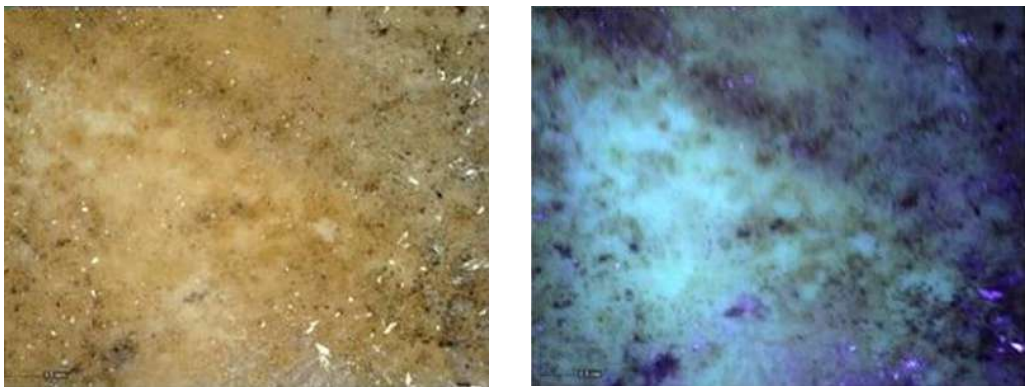

(**a**) (**b**)

Figure 15. Dino-Lite acquisition of the salts with a clear appearance present on the cranium's surface (220×): (**a**) images in visible light; and (**b**) UV fluorescence micrographs.

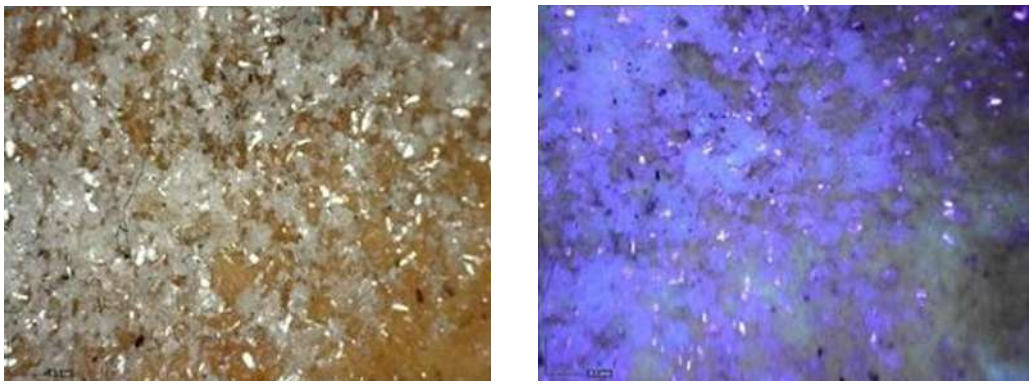

(**a**) (**b**)

Figure 16. Dino-Lite acquisition of the salts with a clear appearance present on the cranium's left side (220×): (**a**) image in visible light; and (**b**) UV fluorescence micrographs.

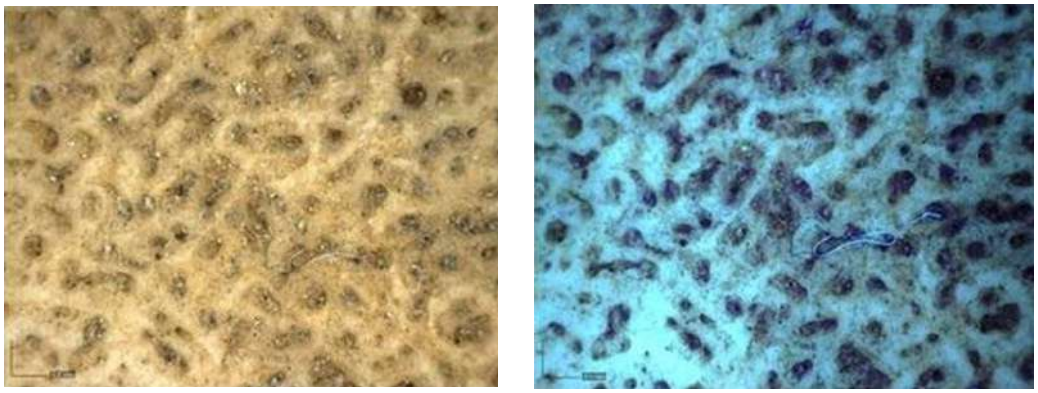

(**a**) (**b**)

Figure 17. Dino-Lite acquisition of the porosities in the outer table of the cranial vault (porotic hyperostosis) (220×): (**a**) image in visible light; and (**b**) UV fluorescence micrographs.

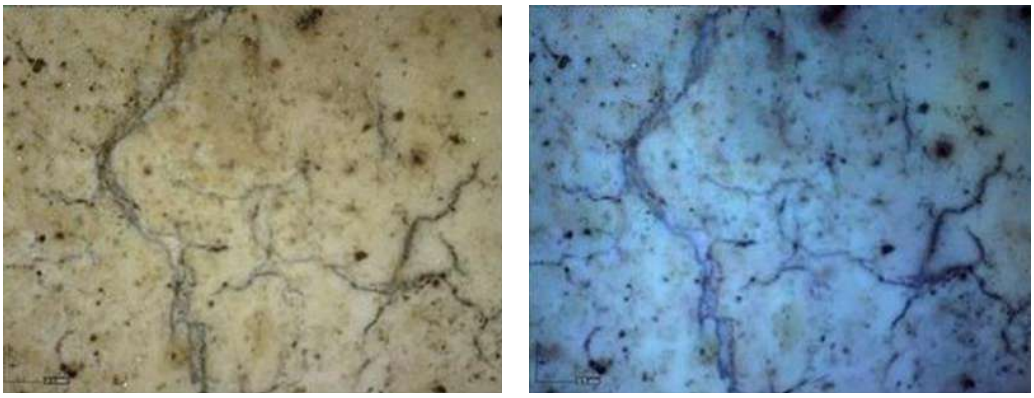

(**a**) (**b**)

Figure 18. Dino-Lite acquisition of the porosities in the orbital roof (cribra orbitalia) (220×): (**a**) image in visible light; and (**b**) UV fluorescence micrographs.

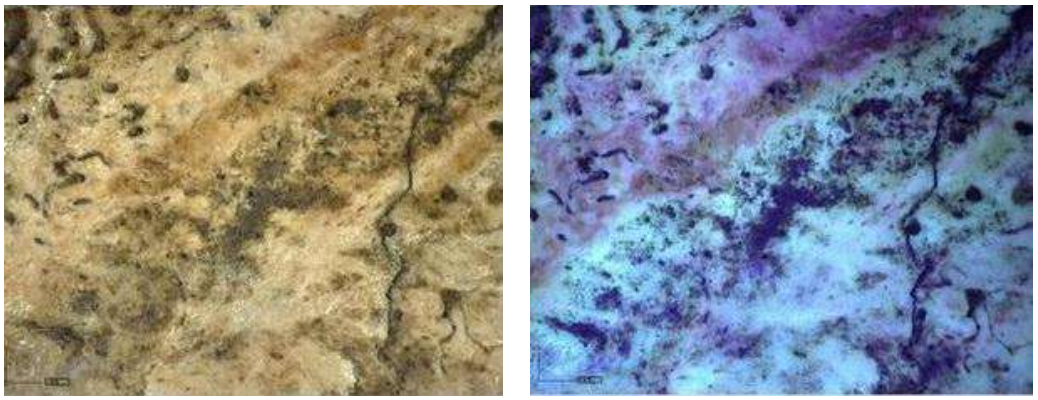

(**a**) (**b**)

Figure 19. Dino-Lite acquisition of the attachment of the temporal muscle (220×): (**a**) image in visible light; and (**b**) UV fluorescence micrographs.

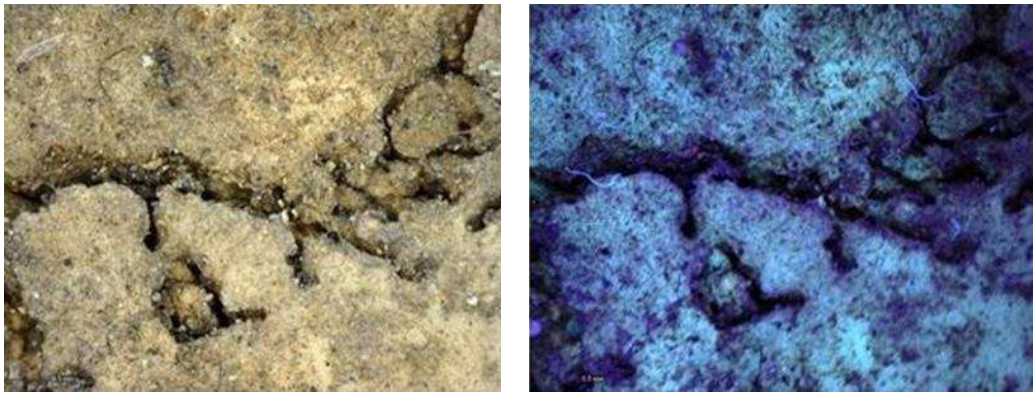

(**a**) (**b**)

Figure 20. Dino-Lite acquisition of the ectocranial tract of the lambdoid suture (220×): (**a**) image in visible light; and (**b**) UV fluorescence micrographs.

(a) Spongy bone

The SEM image shows a low degree of degradation on the spongy tissue and the presence of several fractures that define a fragile bone structure (Figure 21). The chemical analyses highlight the typical elements of the inorganic fraction of the bone tissue, which could identify calcium hydroxyapatite $Ca_5(PO_4)_3(OH)$ (Table 1). These analyses show the presence of minor elements such as Cl, Na, and Al, which are related to salt efflorescence and pollutants. Any residual organic fraction present in the sample was assessed through FTIR-ATR spectroscopy (Section FTIR-ATR Spectroscopy).

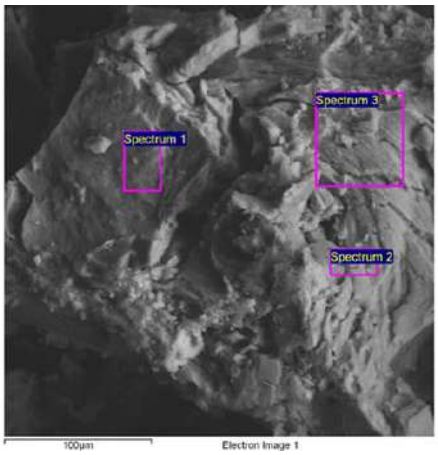

Figure 21. SEM image obtained by energy dispersive X-ray spectrometer (EDS) of the spongy bone.

Table 1. SEM/EDS analysis of the spongy bone.

Spectrum	O *	Na *	Al *	P *	S *	Cl *	Ca *
1	53.8	1	—	16.7	0.4	0.3	27.9
2	44.5	—	1.6	14.3	0.4	0.5	38.7
3	58.7	—	—	13.7	—	—	27.6

* Weight-normalized (wt %). Standard error: ±0.2.

(b) Compact bone

The SEM image and EDS analyses that were carried out on the compact bone show a higher phosphorus (P) content compared to the spongy tissue, which could indicate the recrystallization of the spongy components (Figure 22 and Table 2). Furthermore, the presence of S and Ca is probably related to the traces of calcium sulfate ($CaSO_4$), while

Si and Al might be linked to the environmental pollution and soil. The microstructure of the compact bone shows a high porosity, consisting of irregular holes ranging in size between 30–70 µm, which is probably induced by leaching phenomena, which have erased the traces of the original porosity.

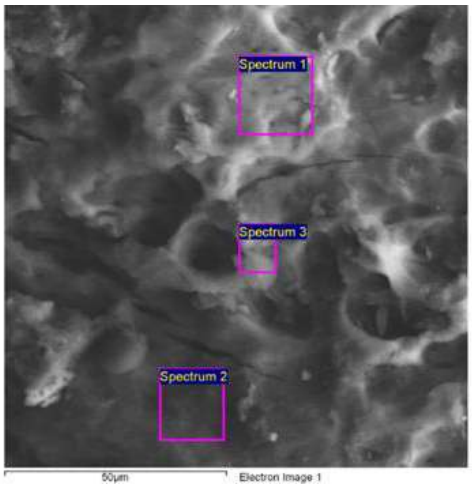

Figure 22. SEM image obtained by energy dispersive X-ray spectrometer (EDS) of the compact part of the bone tissue.

Table 2. EDS analysis of the compact part of the bone tissue.

Spectrum	O *	Na *	Al *	Si *	P *	S *	Cl *	Ca *
1	46.9	0.8	0.4	—	17.8	0.3	0.3	33.6
2	40.5	0.6	0.3	—	17.3	0.3	—	39.7
3	40.4	0.9	0.4	0.6	18.1	1.2	—	38.8

* Weight-normalized (wt %). Standard error: ±0.2.

(c) Salt efflorescence

The SEM micrograph of the saline efflorescence highlights the formation of second-generation large crystals, which is related to a slow crystallization process (Figure 23).

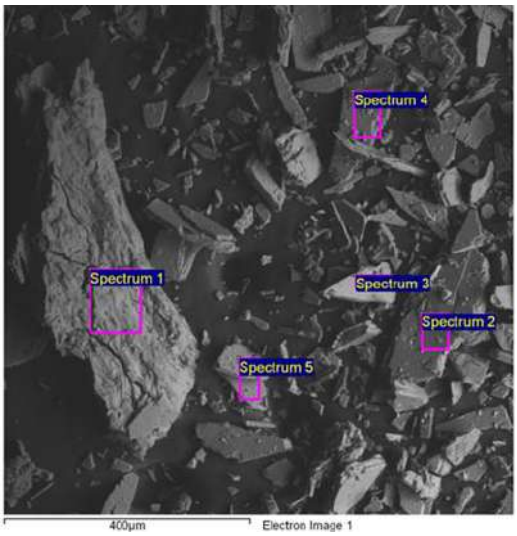

Figure 23. SEM image obtained by energy dispersive X-ray spectrometer (EDS) of the compact part of the salts.

The EDS analysis of the salts that were sampled from the skull's external surface shows the presence of Ca, S, and P, highlighting the possible presence of recrystallized hydroxyapatite (Ca and P) and gypsum (Ca and S) (Table 3).

Table 3. EDS analysis of the compact part of the salts.

Spectrum	C *	O *	Na *	P *	S *	Cl *	Ca *
1	—	53.4	0.8	14.5	1.3	0.3	29.7
2	—	63.7	—	15.8	1.4	—	19.1
3	7.5	61.1	—	13.7	1.4	—	16.4
4	9.1	58.2	—	15.1	0.3	—	17.4
5	8.7	60.9	—	13.4	0.4	—	16.1

* Weight-normalized (wt %). Standard error: ±0.2.

(d) Dark patina

The EDS analyses of the dark patina that was visible on the shelf highlight the typical elements of a silico-cementitious stucco (a high content of Si, Ca, Fe, and Al) and calcium sulfate, which is related to the constituent materials of the surrounding environment (Figure 24 and Table 4). In addition, the presence of Mg, Si, Fe, Al, and K may be linked to the aluminosilicates present in the surroundings of the skull's deposition site.

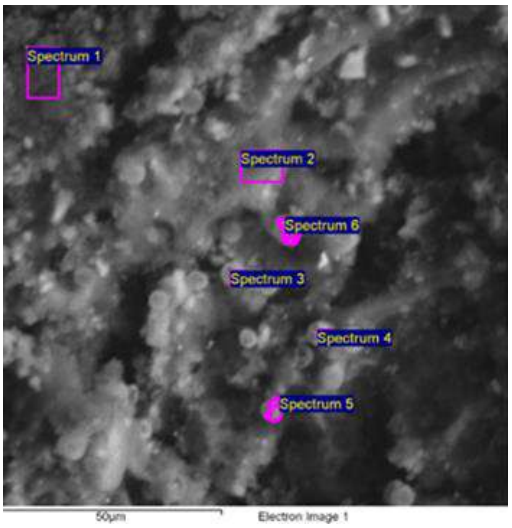

Figure 24. SEM image obtained by energy dispersive X-ray spectrometer (EDS) of the dark patina present on the shelf.

Table 4. EDS analysis of the compact part of the dark patina present on the shelf.

Spectrum	O *	Mg *	Al *	Si *	P *	S *	Cl *	K *	Ca *	Fe *
1	15.6	—	—	0.6	—	0.9		0.5	82.4	—
2	57.3	—	1.3	3.4	0.7	1.2	0.6	3.8	26.5	3.2
3	53.6	—	1	2.4	—	0.6	—	1.1	38.8	2.4
4	65.2	0.7	0.6	2.1	—	0.4	—	0.4	29.6	0.4
5	64.0	0.7	0.8	1.8	—	0.9	0.3	0.6	30.1	0.7
6	52.1	—	1	2	0.4	1.7	—	1.1	40.4	1.3

* Weight-normalized (wt %). Standard error: ±0.2.

The SEM image that was acquired from the same sample, which can be seen in Figure 24, shows the presence of spherical structures that can be related to the fungal species responsible for the black coloring of the cranium surface, when observed at a higher magnification (Figure 25 and Table 5) [30,31].

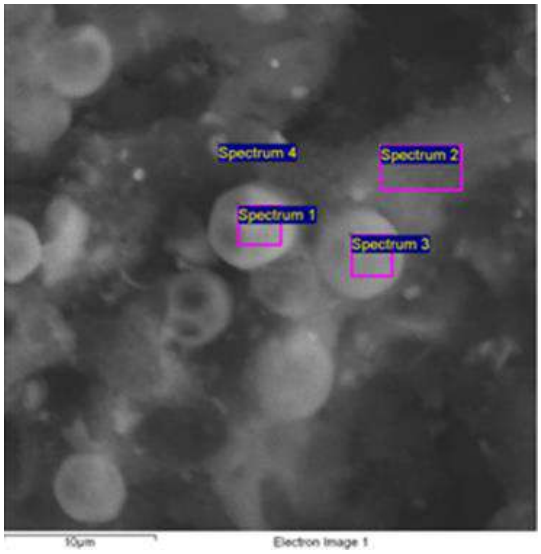

Figure 25. SEM image and chemical analyses obtained by energy dispersive X-ray spectrometer (EDS) of the fungal species responsible for the black coloring of the material.

Table 5. EDS analysis of the fungal species responsible for the black coloring of the material. The element carbon understands the contribution of other elements.

Spectrum	O *	Mg *	Al *	Si *	S *	Cl *	K *	Ca *	Fe *
1	58.3	0.5	0.6	2.1	5.5	2.0	0.6	28.8	0.4
2	54.3	0.9	1.0	3.4	1.3	0.7	2.8	30.7	4.7
3	61.6	0.7	0.5	1.6	0.4	—	0.5	33.8	0.8
4	39.8	—	0.8	2.3	—	—	1.8	46.6	8.4

* Weight-normalized (wt %). Standard error: ±0.2.

FTIR ATR Spectroscopy

FTIR spectroscopy was carried out on the salts that were taken from the surface of the cranium and the shelf. Figure 26 shows the spectrum that was collected by this investigation of the cranium salts.

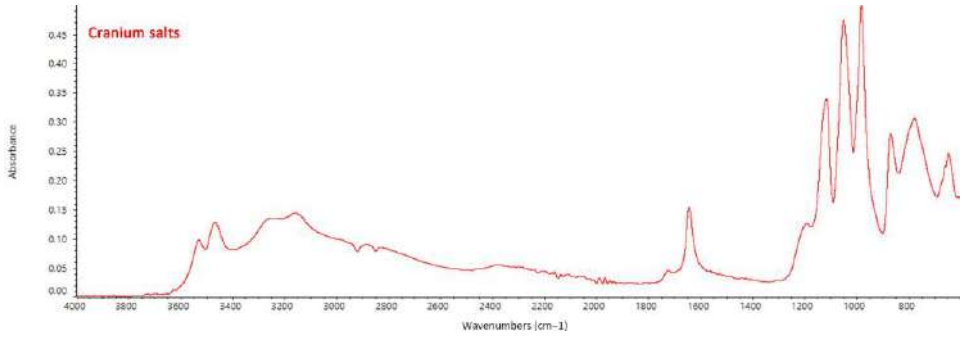

Figure 26. FTIR-ATR spectrum of hydroxyapatite presents on the skull.

In the spectrum, it is possible to identify the main hydroxyapatite $Ca_{10}(PO_4)_6(OH)_2$ bands. The peak at 640 cm^{-1} is related to the asymmetric bending vibration of the phosphate group (υ_4 PO_4^{3-}). The bands at 982 and 2900 cm^{-1} can be, respectively, linked to the P-O symmetric stretching and (P-)O-H stretching of HPO_4^{2-} [32,33]. The peak at 1048 cm^{-1} can be assigned to the asymmetric stretching (υ_3 PO_4^{3-}), while the peak at 1113 cm^{-1} to the PO_4^{3-} asymmetric stretching in stoichiometric apatite [34,35]. The band at 1192 cm^{-1} can be attributed to the asymmetric stretching vibration of HPO_4^{2-} [36], while the one at

870 cm^{-1} is associated with the υ_2 symmetric stretching vibrations of carbonate ions, which can be incorporated into the apatites from atmospheric CO_2 [32]. The peak at 3338 cm^{-1} corresponds to the ion stretching of the OH^-, confirming the presence of the hydroxyl group, while the water that is associated with hydroxyapatite can be seen at 3471 and 1641 cm^{-1}, respectively, corresponding to the stretching and bending vibrations [37–39]. These FT-IR ATR analyses could have detected vestigial organic fractions in the samples, such as collagen. However, no bands related to amide groups can be noticed.

Figure 27 shows the IR spectrum of the whitish salts that were taken from the shelf's surface. The characteristic bands of the gypsum ($CaSO_4 \cdot 2H_2O$) constituting the shelf can be observed. No peaks associated with the salts that were present on the cranium are detected.

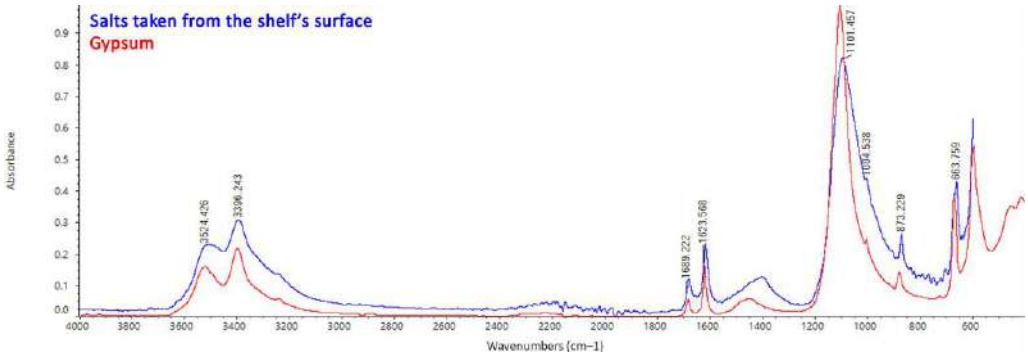

Figure 27. FTIR-ATR spectrum of the salts samples from the site of collocation of the skull, i.e., the shelf's surface (blue line), compared with the spectrum of gypsum (red line).

Microbiological Testing

The microbiological examinations that were performed on the surface revealed the presence of fungi with environmental origins (Figure 28). This analysis allowed for the detection of microorganisms' presence, but not for the isolation of their specific types. Tests that were aimed at defining the bacterial load highlighted the growth of bacteria that were related to environmental microbial contamination at around 22 °C. Bacteria related to a contamination of human or animal origin—which grow at around 37 °C—were not reported.

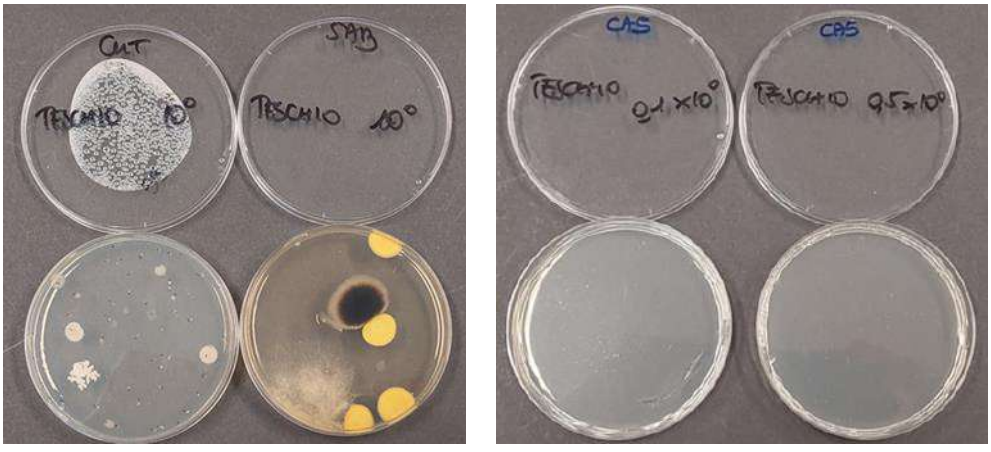

(**a**) (**b**)

Figure 28. (**a**) Bacterial Culture Test (CUT): plate agar for the total bacterial count. SAB: Saboraud Dextrose agar for the total fungal count. (**b**) CAS: cetrimide agar for research and counts of *Pseudomonas aeruginosa*.

The Sabouraud CAF Agar allowed for the identification of the fungal species that were present on the cranium's surface, which mainly consisted of *Penicillium* and *Ulocladium*,

of environmental origin. Their presence was linked to the continuous exchange with the outdoor environment and the high relative humidity (RH%) in the crypt.

Further tests were performed on the cetrimide agar to observe the growth of *Pseudomonas aeruginosa*, which provided a negative outcome. Even though the environment was contaminated by microorganisms, it was possible to exclude the presence of the most common Gram-negative pathogen for humans, i.e., *Pseudomonas aeruginosa.*

Radiographic Images

Radiographic images were collected on three sides of the cranium to determine the presence of eventual micro-fractures, whose identification through microscopical observations would have been difficult.

The radiographs (Figure 29) show no further severe damage to the skull. Some anatomical features are visible, including the complex morphology of the frontal sinuses, the increased thickness of the diploe, and the vascular impressions on the parietal bones.

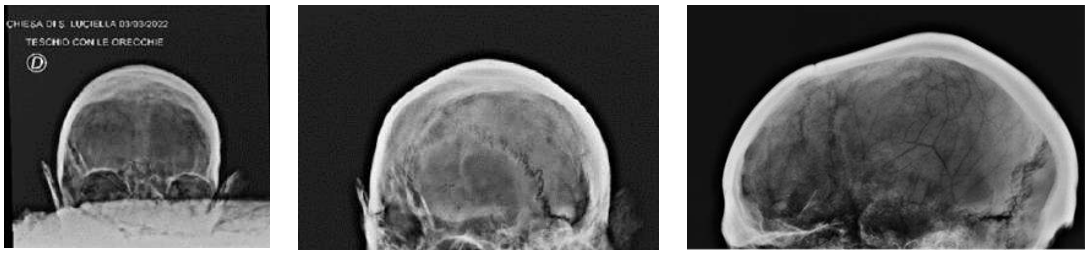

(**a**) (**b**) (**c**)

Figure 29. Radiographic images of the cranium: (**a**) front, (**b**) back, and (**c**) lateral views.

Radiocarbon Dating

The results of the radiocarbon dating and stable isotope measurements are shown in Table 6 and Figure 30.

Table 6. Radiocarbon dating. Tcr: tree-ring corrected. BP: before present. PDB: Pee Dee Belemnite.

Sample	Lab. Code	Trc (Years BP)	Calendarial Age AD (2σ)	$\delta^{13}C$ vs. PDB (per Mil)	$\delta^{15}N$ vs. AIR (per Mil)
Bone tissue (Skull with ears)	DSH11416-icon25	120 ± 22	Modern	−20.7	8.4

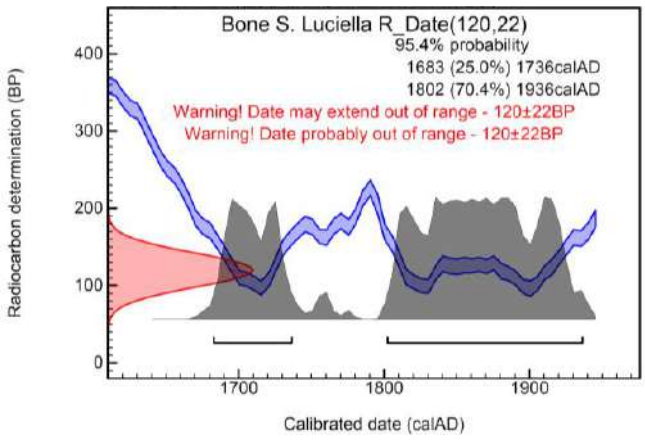

Figure 30. Calibration of radiocarbon.

The calibration of the radiocarbon measurements showed different possible dating ranges, but it appears to be more plausible that it falls in a modern range of age—i.e., from 1850 AD—while it is less likely to be in an age interval of the range 1683–1736 AD.

3.3. First Aid Treatment

The first aid intervention started with the preparation of the area, which consisted of the temporary removal of the sediments and bone fragments of the other finds from the shelf.

Afterward, cleaning tests were performed on the surface of the cranium, starting with the gentle removal of the dust and incoherent deposits from the unaltered surface by using soft brushes.

Due to the sensitivity of the bone tissue to water, the humid cleaning tests to remove the saline aggregates and coherent deposits were performed with organic solutions (alcohol and acetone), and gently rubbed onto the surface with cotton buds (Figure 31).

(**a**) (**b**)

Figure 31. Images of the cranium (**a**) during, and (**b**) after the cleaning procedure.

In order to move the cranium and treat the posterior and lower parts, local consolidations were performed using an acrylic consolidant with increasing concentrations. Paraloid B72® in acetone was used in the concentrations of 2%, 3%, 5%, and 10% (*w*/*v*), based on the conservation state and porosity of the bone tissue.

Due to their fragility, great attention was paid to the consolidation of the temporal bones, the squamous suture, and the lambdoid suture, to stabilize both the bone tissue and the suture.

Once they were dried, the bone fragments that remained attached to the stone because of the coherent salt encrustations were documented and cataloged. The cranium was then placed upside down on a shaped Ethafoam support, to allow for the treatment of the basal part with repeated applications of acrylic resin (Figures 32 and 33).

(**a**) (**b**)

Figure 32. Operations to secure the cranium: consolidation work (**a**,**b**).

(**a**) (**b**)

Figure 33. Operations to secure the cranium: consolidation work (**a**,**b**).

After applying an acrylic-based sacrificial layer, namely Paraloid B72® in a concentration of 10% w/v in acetone, which ensures the reversibility of the application, the fragments that were partially detached from the basal part of the cranium were stabilized by drops of an instant acrylic adhesive (Super At-tak®-Loctite).

The aforementioned detached fragments were consolidated with Paraloid B72® in a concentration of 5% (w/v) in acetone. Those that were impossible to replace on the cranium were wrapped in tissue paper and placed inside the crypt in a breathable container.

The weight of the cranium was centered on the left nasal bone during the years of its exposition on the shelf. For this reason, it appeared to be in an advanced state of decohesion, showing fractures and detachments from the frontal bone. Thus, both the nasal bones were carefully cleaned and consolidated (Ibid), especially along the sutures that were connected to the frontal bone. The attachment points were identified, and the nasal bones were welded to the frontal bone with a polyvinyl ester adhesive, namely UHU extra®—UHU GmbH & Co. (Bühl, Germany) (Figures 34 and 35). The same procedure was repeated for all the fragments with 100% recognizable joints.

(**a**) (**b**)

Figure 34. Relocation of the bones and detached fragments: nasal bones repositioning and gluing (**a**), and nasal bones following the procedure (**b**).

The securing intervention was completed with the creation of a temporary structure to support the cranium during its exposure, aimed at separating the object from the shelf. It will also allow for the safe manipulation of the cranium in its future monitoring and interventions.

(**a**) (**b**)

Figure 35. Relocation of the bones and detached fragments: fragments relocation in the basal and temporal part (**a**), and the base of the cranium after the intervention (**b**).

The support was composed of three different elements that were made of polymethylmethacrylate: a flat and square element of 20 × 20 cm and two arcuate pillars, assembled to keep the cranium's weight off the nasal bones, which were severely degraded. The contact areas of both the plate and the two pins were coated with a 0.5 mm layer of expanded polyethylene to prevent cracking and slippage. The two pins were meant to slightly raise the cranium, so that the nasal bones did not touch the plate, while distributing the weight onto the orbital bones instead, which were in good condition (Figures 36 and 37).

(**a**) (**b**)

Figure 36. Construction of temporary support for the cranium (**a**,**b**).

(**a**) (**b**)

Figure 37. Placement of the "Skull with ears" on the support (**a**,**b**).

A consolidation and plastering procedure for the shelf preceded the relocation of the cranium to its original location. A lime–sand mortar was used to reintegrate the deep fracture that was present in the area of the collocation of the cranium, while the neighboring bone fragments, which were removed before the intervention, were returned to their original positions (Figures 38–40).

(**a**) (**b**)

Figure 38. In situ relocation of the "Cranium with ears" to its original site: right (**a**), and left (**b**) sides.

(**a**) (**b**)

Figure 39. In situ relocation of the "Skull with ears" to its original site: view from the top (**a**), and front view (**b**).

Figure 40. In situ relocation of the "Cranium with ears" to its original site: overall view.

Eventually, clay was used to reversibly attach the support to the shelf, thus securing it and preventing top slippage.

4. Discussion

The "Skull with Ears" intercepts two important cultural phenomena that have been consolidated and stratified within the historical Neapolitan culture over the centuries. The placement of this and the other skulls on the shelves located inside the crypt of Santa Luciella's church represents the final act of a multistage process of the guided decomposition of bodies. This corpse treatment has a strong symbolic meaning. It occurred in numerous *terresante* beneath Naples' churches and was run by secular fraternities or religious orders.

Over time, the remains in Santa Luciella's church have eventually lost their identities and direct relationships with the deceased, but in their becoming anonymous, they have emerged as protagonists in a different, well-rooted phenomenon of Neapolitan tradition: the cult of "Abandoned Souls".

The diagenetically altered temporal bones of the "Skull with ears" were indeed long mistaken to be mummified ears. Thus, devotees thought that this prodigious phenomenon charged the skull with a greater mediatic power between the world of the living and the world of the dead.

For these reasons, the "Skull with ears" now represents a material expression of popular historical customs and shared cultural identity; as such, it should be preserved and maintained for future generations [40].

The climatic conditions of the hypogeum required an intervention to secure the skull through a multi-step process. It was preceded by in-depth diagnostic analyses to identify the environmental criticalities and ongoing diagenetic processes acting on the bones, in order to implement a suitable and decisive conservation strategy.

The microclimatic measurements showed extremely high values of relative humidity (RH%) ($98 \pm 1\%$) and a temperature of 16 ± 2 °C.

The procedures directly involving the cranium—i.e., the sampling, documentation, and first aid treatment—were carried out by maintaining it on its site of collocation.

The macroscopical observations in the UV light and the Dino-Lite images revealed the existence of coherent and incoherent deposits on the cranium's surface. The images that were acquired on the surface by using the digital microscope highlighted the presence of white/grey inorganic aggregates and transparent and colorless salts, with no fluorescence emission under UV radiation.

Electron scanning microscopy (SEM), coupled with energy dispersive spectroscopy (EDS), showed the main differences between the spongy tissue and the compact bone. Specifically, the compact bone showed a higher content of phosphorus (P), which could indicate the recrystallization of the spongy components. Both the spongy tissue and the compact bone showed the presence of minor elements related to salt efflorescence and pollutants. Additionally, the analysis of the saline efflorescence highlighted the possible presence of recrystallized hydroxyapatite (Ca and P) and gypsum (Ca), while the SEM micrograph showed the formation of second-generation large crystals, which was related to a slow crystallization process. The sample consisting of the dark patina that was present on the shelf contained the typical elements of a silico-cementitious stucco (high content of Si, Ca, Fe, Al) and calcium sulfate, which were related, respectively, to the constituent materials of the shelf and the surrounding environment.

The FTIR-ATR analyses that were performed on the salts sampled from the cranium resulted in a spectrum that was comparable to that of the hydroxyapatite, having large crystals. The deposit that was taken from the shelf's surface was identified as gypsum, which was related to the constituent materials of the surrounding structure.

The microbiological examinations performed on the dark patina that was visible on the cranium's surface only revealed the presence of fungi with environmental origins, which are not pathogenic to humans. They mainly consisted of *Penicillium* and *Ulocladium* of environmental origin, presumably due to both the high degree of relative humidity in the crypt and the exchange with the outdoor environment.

The 3D documentation allowed for the direct reporting of all the data that were related to the cranium's conservation status on its 3D model, as well as the operations performed during the intervention. The comparison between the 3D models that were realized before and after the first aid intervention allowed for the understanding of the aesthetic consequences of the consolidation treatment on the cranium.

The operations of the find were guided by the principle of "minimum intervention" and consisted of the restoration of the material's cohesive properties—in particular in the "ears" area—and the realization of a temporary support for avoiding direct contact between the cranium and the shelf. To pursue this goal, several materials were tested in the

laboratory to find the most suitable ones for the environment of the crypt and its peculiar micro-climatic features.

The support that was created during the intervention will preserve the cranium in the short term, but it needs to be replaced by a new support consisting of an internal structure that is calibrated according to the morphological and structural characteristics of the cranium.

5. Conclusions

The "Skull with Ears" belonged to an adult male who died in the 19th century. For its peculiar aspect of deformed and detached temporal bones that resemble mummified ears, the skull has become a cult object and an expression of cultural identity that is embedded in Neapolitan popular customs.

The diagnostic investigation enabled the acquisition of significant information on the taphonomical and anthropological features of the cranium, while identifying the constituent components of the salts that were present on its surface. The analyses also allowed for the definition of the conservation states of the finds. They revealed the advanced state of degradation of the bones due to a significant bacterial attack, which was facilitated by the inadequate environmental conditions (98% RH) of the site of conservation.

The first aid intervention was performed entirely on-site to prevent any risk of further damage. A temporary support was developed to provisionally secure the cranium—which showed an extensive fragmentation of the nasal bones before the intervention—while maintaining it in its original location. The support will be replaced in the future with a permanent structure, which will be optimized according to the morphological and structural parameters of the cranium. This definitive support will be developed based on the 3D reconstruction, thus avoiding any direct manipulations of the original find.

The future monitoring of the microclimatic parameters and their effects on all the bones remains present in the crypt and will be essential for defining the most suitable preservation approach, by stabilizing the environmental parameters of the crypt while preserving its symbolic value.

Author Contributions: Conceptualization, A.M., M.F. and A.S.; methodology, A.M., S.M. and E.C.; validation, A.M. and T.d.C.; investigation, C.B., G.S., C.V., R.A. and M.R.D.C.; resources A.M., M.F., C.L. and A.R.; data curation, G.S., A.M. and A.A.; writing—original draft preparation, A.M., T.d.C., E.C., G.S. and A.S.; writing—review and editing, G.S. and C.B.; supervision, A.M.; project administration, M.F. and A.R. All authors have read and agreed to the published version of the manuscript.

Funding: This research was funded by Respiriamo Arte (Vico Santa Luciella ai Librai 5, 80138 Naples, Italy) in collaboration with Round Table Italia, and Round Table Napoli (Via Cisterna dell'Olio 44, 80134 Naples, Italy).

Acknowledgments: Thanks to Respiriamo l'Arte, Artes Restauro e Servizi per l'Arte, Round Table Italia, and Round Table Napoli Organisations for supporting the project.

Conflicts of Interest: The authors declare no conflict of interest.

References

1. Larson, F. *Severed: A History of Heads Found*; Granta Books: London, UK, 2015.
2. D'Agostino, E.; Sperduti, A. Skulls. Antenati, Santi e Nemici. In *Avo Sapiens. Immagini Dall'oltre Mondo*; La Lepre Edizioni: Rome, Italy, 2022; pp. 108–122.
3. Maiello, G. An Extreme and Massive Expression of the Iconization of Suffering: The Cult of the "Abandoned Souls" in Naples. In *The Iconization of Suffering in Literary and Interdisciplinary Perspectives*; Constantine the Philosopher University: Nitra, Slovakia, 2019; pp. 145–154.
4. De Matteis, S. From the anonymous skulls to the collective trance. Ritual representation in the neapolitan underclass. *Illuminazioni* **2019**, *48*, 206–277.
5. Guarino, M. Secondary burials in Naples in the modern and contemporary age: A review. *Ethics Med. Public Health* **2022**, *22*, 100793. [CrossRef]
6. Guarino, M. The hypogea of the churches of Naples: Burials and cult of the dead. *Pap. Anthropol.* **2022**, *31*, 7–34. [CrossRef]
7. Van Gennep, A. *The Rites of Passage*; The University Press of Chicago: Chicago, IL, USA, 1966.

8. Vetromile, C.; Spagnuolo, A.; Petraglia, A.; Masiello, A.; di Cicco, M.R.; Lubritto, C. Pre- and post-operam comparison of the energy consumption of a radio base station under energy efficiency actions. *Energy Build.* **2021**, *236*, 110772. [CrossRef]
9. Spagnuolo, A.; Vetromile, C.; Masiello, A.; Alberghina, M.F.; Schiavone, S.; Di Cicco, M.R.; Formato, R.; Lubritto, C. RE-SEMIRTO project: An innovative network of wireless sensors for microclimate monitoring on the Royal Palace of Carditello. *J. Phys. Conf. Ser.* **2022**, *2204*, 012076. [CrossRef]
10. D'Agostino, D.; Macchia, A.; Cataldo, R.; Campanella, L.; Campbell, A. Microclimate and Salt Crystallization in the Crypt of Lecce's Duomo. *Int. J. Archit. Herit.* **2015**, *9*, 290–299. [CrossRef]
11. Randazzo, L.; Ricca, M.; Pellegrino, D.; La Russa, D.; Macchia, A.; Rivaroli, L.; Marrone, L.; Enei, F.; La Russa, M.F. Anti-fouling additives for the consolidation of archaeological mortars in underwater environment: Efficacy tests performed on the apsidal fishpond of castrumnovum (Rome, Italy). *Int. J. Conserv. Sci.* **2020**, *11*, 243–250.
12. Macchia, A.; Bettucci, O.; Gravagna, E.; Ferro, D.; Albini, R.; Mazzei, B.; Campanella, L. Calcium Hydroxide Nanoparticles and Hypogeum Environment: Test to Understand the Best Way of Application. *J. Nanomater.* **2014**, *2014*, 167540. [CrossRef]
13. Biehler-Gomez, L.; Porta, D.; Mattia, M.; De Angelis, D.; Poppa, P.; Cattaneo, C. 'Ye must have faith' how anthropology can contribute to religious heritage: The osteobiography of Italian martyr Saint Nazarius. *Int. J. Osteoarchaeol.* **2021**, *31*, 506–512. [CrossRef]
14. Ministero della Cultura. *I Resti Scheletrici Umani: Dallo Scavo, al Laboratorio, al Museo*; Istituto Centrale per il Catalogo e la Documentazione/Istituto Centrale per l'Archeologia: Roma, Italy, 2022.
15. Swaraldahab, M.A.H.; Christensen, A.M. The Effect of Time on Bone Fluorescence: Implications for Using Alternate Light Sources to Search for Skeletal Remains. *J. Forensic Sci.* **2016**, *61*, 442–444. [CrossRef]
16. Macchia, A.; Biribicchi, C.; Carnazza, P.; Montorsi, S.; Sangiorgi, N.; Demasi, G.; Prestileo, F.; Cerafogli, E.; Colasanti, I.A.; Aureli, H.; et al. Multi-Analytical Investigation of the Oil Painting "Il Venditore di Cerini" by Antonio Mancini and Definition of the Best Green Cleaning Treatment. *Sustainability* **2022**, *14*, 3972. [CrossRef]
17. Macchia, A.; Biribicchi, C.; Rivaroli, L.; Aureli, H.; Cerafogli, E.; Colasanti, I.A.; Carnazza, P.; Demasi, G.; La Russa, M.F. Combined Use of Non-Invasive and Micro-Invasive Analytical Investigations to Understand the State of Conservation and the Causes of Degradation of I Tesori del Mare (1901) by Plinio Nomellini. *Methods Protoc.* **2022**, *5*, 52. [CrossRef]
18. Spagnolo, A.M.; Santini, M.; Cristina, M.L. *Pseudomonas aeruginosa* in the healthcare facility setting. *Rev. Med. Microbiol.* **2021**, *32*, 169–175. [CrossRef]
19. Planet, P.J. Pseudomonas aeruginosa. In *Principles and Practice of Pediatric Infectious Diseases*; Elsevier: Amsterdam, The Netherlands, 2023; pp. 884–889.
20. Longin, R. New method of collagen extraction for radiocarbon dating. *Nature* **1971**, *230*, 241–242. [CrossRef] [PubMed]
21. DeNiro, M.J. Postmortem preservation and alteration of in vivo bone collagen isotope ratios in relation to palaeodietary reconstruction. *Nature* **1985**, *317*, 806–809. [CrossRef]
22. Pate, F.D. Bone chemistry and paleodiet. *J. Archaeol. Method Theory* **1994**, *1*, 161–209. [CrossRef]
23. Van Klinken, G.J. Bone collagen quality indicators for palaeodietary and radiocarbon measurements. *J. Archaeol. Sci.* **1999**, *26*, 687–695. [CrossRef]
24. Ramsey, C.B.; Heaton, T.J.; Schlolaut, G.; Staff, R.A.; Bryant, C.L.; Brauer, A.; Lamb, H.F.; Marshall, M.H.; Nakagawa, T. Reanalysis of the athmospheric radiocarbon calibration record from Lake Suigetsu, Japan. *Raiocarbon* **2020**, *62*, 989–999. [CrossRef]
25. Reimer, P.; Austin, W.; Bard, E.; Bayliss, A.; Blackwell, P.; Ramsey, C.B.; Talamo, S. The IntCal20 northern hemisphere radiocarbon age calibration curve (0–55 cal kBP). *Radiocarbon* **2020**, *62*, 725–757. [CrossRef]
26. Buikstra, J.E.; Ubelaker, D.H. Standards for data collection from human skeletal remains. *Ark. Archaeol. Surv. Res. Ser.* **1994**, *44*. [CrossRef]
27. Lovejoy, C.O. Dental wear in the Libben population: Its functional pattern and role in the determination of adult skeletal age at death. *Am. J. Phys. Anthropol.* **1985**, *68*, 47–56. [CrossRef]
28. Rivera, F.; Lahr, M.M. New evidence suggesting a dissociated etiology for cribra orbitalia and porotic hyperostosis. *Am. J. Phys. Anthropol.* **2017**, *164*, 76–96. [CrossRef] [PubMed]
29. Bonora, V.; Tucci, G.; Meucci, A.; Pagnini, B. Photogrammetry and 3D Printing for Marble Statues Replicas: Critical Issues and Assessment. *Sustainability* **2021**, *13*, 680. [CrossRef]
30. Alves, E.; Lucas, G.C.; Pozza, E.A.; de Carvalho Alves, M. Scanning Electron Microscopy for Fungal Sample Examination. *Lab. Protoc. Fungal Biol.* **2013**, 133–150. [CrossRef]
31. Beech, I.; Otlewska, A.; Skòra, J.; Gutarowska, B.; Gaylarde, C. Interactions of fungi with titanium dioxide from paint coating. *Indoor Built Environ.* **2018**, *27*, 263–269. [CrossRef]
32. Pleshko, N.; Boskey, A.; Mendelsohn, R. Novel infrared spectroscopic method for the determination of crystallinity of hydroxyapatite minerals. *Biophys. J.* **1991**, *60*, 786–793. [CrossRef] [PubMed]
33. Katić, J.; Krivačić, S.; Petrović, Ž.; Mikić, D.; Marciuš, M. Titanium Implant Alloy Modified by Electrochemically Deposited Functional Bioactive Calcium Phosphate Coatings. *Coatings* **2023**, *13*, 640. [CrossRef]
34. Iconaru, S.; Motelica-Heino, M.; Predoi, D. Study on Europium Doped Hydroxyapatite Nanoparticles by Fourier Transform Infrared Spectroscopy and Their Antimicrobial Properties. *J. Spectrosc.* **2013**, *2013*, 284285. [CrossRef]

35. Vechietti, F.A.; Marques, D.; Muniz, N.O.; Santos, L.A. Fibers Obtaining and Characterization Using Poly (Lactic-co-Glycolic Acid) and Poly (Isoprene) Containing Hydroxyapatite and α TCP Calcium Phosphate by Electrospinning Method. *Key Eng. Mater.* **2015**, *631*, 173–178. [CrossRef]
36. Dritsa, V.; Pissaridi, K.; Koutoulakis, E.; Mamarelis, I.; Kotoulas, C.; Anastassopoulou, J. An Infrared Spectroscopic Study of Aortic Valve. A Possible Mechanism of Calcification and the Role of Magnesium Salts. *In Vivo* **2014**, *28*, 91–98.
37. Chandrasekaran, A.; Sagadevan, S.; Dakshanamoorthy, A. Synthesis and characterization of nano-hydroxyapatite (n-HAP) using the wet chemical technique. *Int. J. Phys. Sci.* **2013**, *8*, 1639–1645.
38. Cengiz, B.; Gokce, Y.; Yildiz, N.; Aktas, Z.; Calimli, A. Synthesis and characterization of hydroxyapatite nanoparticles. *Colloids Surf. A Physicochem. Eng. Asp.* **2008**, *322*, 29–33. [CrossRef]
39. Kesmez, O. Preparation of Anti-bacterial Biocomposite Nanofibers Fabricated by Electrospinning Method. *J. Turk. Chem. Soc. A* **2020**, *7*, 125–142. [CrossRef]
40. Council of Europe (CoE). Council of Europe Framework Convention on the Value of Cultural Heritage for Society. In Faro Declaration of the Council of Europe's Strategy for Developing Intercultural Dialogue. 2005. Available online: https://rm.coe.int/1680083746 (accessed on 27 January 2023).